

Article

Antifungal Action of Metallic Nanoparticles Against Fungicide-Resistant Pathogens Causing Main Postharvest Lemon Diseases

Carina G. Baigorria ¹, Luciana Cerioni ¹, Mario A. Debes ^{1,2} , Ana E. Ledesma ³ , Patricio Alastuey ⁴ ,
Mónica Tirado ⁴ , Sabrina I. Volentini ^{1,*}  and Viviana A. Rapisarda ^{1,*} 

- ¹ Instituto Superior de Investigaciones Biológicas (INSIBIO), CONICET-UNT, and Instituto de Química Biológica “Dr. Bernabé Bloy”, Facultad de Bioquímica, Química y Farmacia, UNT, San Miguel de Tucumán 4000, Argentina
- ² Cátedra de Anatomía Vegetal, Facultad de Ciencias Naturales e Instituto Miguel Lillo, UNT, San Miguel de Tucumán 4000, Argentina
- ³ Centro de Investigación en Biofísica Aplicada y Alimentos (CIBAAL), CONICET-UNSE, Santiago del Estero 4206, Argentina
- ⁴ Instituto de Física del Noroeste Argentino (INFINOA), CONICET-UNT, Facultad de Ciencias Exactas y Tecnología, FACET, UNT, San Miguel de Tucumán 4002, Argentina
- * Correspondence: sabrina.volentini@fbqf.unt.edu.ar (S.I.V.); viviana.rapisarda@fbqf.unt.edu.ar (V.A.R.)

Abstract: Postharvest fungal diseases are the main cause of economic losses in lemon production. The continued use of synthetic fungicides to control the diseases favors the emergence of resistant strains, which encourages the search for alternatives. The aim of this study was to assess the efficacy of metallic nanoparticles (NPs) as antifungal agents against local isolates of *Penicillium digitatum* and *Penicillium italicum*, each of them in a fungicide-sensitive and -resistant version, and a *Geotrichum citri-aurantii* isolate. NPs of ZnO, CuO, and Ag were synthesized and characterized by spectroscopy and microscopy, presenting average sizes < 25 nm and spherical shapes. ZnO-NPs did not present antifungal activity at the assayed conditions, while the minimum fungicidal concentrations (MFCs) were 1000 and 10 µg mL⁻¹ for CuO-NPs and Ag-NPs, respectively. The NPs’ antimicrobial action included conidial membrane permeability and strong intracellular disorganization. Moreover, the Ag-NPs reduced green mold incidence on inoculated lemons when applied to the fruit. Taken together, Ag-NPs were effective in inhibiting both fungicide-sensitive and -resistant isolates of the main lemon postharvest pathogens, suggesting their potential use as an alternative approach.

Keywords: silver nanoparticles; cupric oxide nanoparticles; *Penicillium digitatum*; *Penicillium italicum*; *Geotrichum citri-aurantii*



Citation: Baigorria, C.G.; Cerioni, L.; Debes, M.A.; Ledesma, A.E.; Alastuey, P.; Tirado, M.; Volentini, S.I.; Rapisarda, V.A. Antifungal Action of Metallic Nanoparticles Against Fungicide-Resistant Pathogens Causing Main Postharvest Lemon Diseases. *J. Fungi* **2024**, *10*, 782. <https://doi.org/10.3390/jof10110782>

Academic Editor: Nengguo Tao

Received: 29 August 2024

Revised: 17 October 2024

Accepted: 5 November 2024

Published: 11 November 2024



Copyright: © 2024 by the authors. Licensee MDPI, Basel, Switzerland. This article is an open access article distributed under the terms and conditions of the Creative Commons Attribution (CC BY) license (<https://creativecommons.org/licenses/by/4.0/>).

1. Introduction

Significant economic losses worldwide are generated due to citrus postharvest fungal diseases, which include green and blue molds and sour rot, caused by *Penicillium digitatum*, *Penicillium italicum*, and *Geotrichum citri-aurantii*, respectively [1–3]. Argentina is the world’s sixth largest producer of citrus fruits, and our region, located in the northwest of Argentina, accounts for around 80% of the country’s lemon production [4]. Currently, to control these fungal diseases, a reduced spectrum of fungicides can be applied, such as thiabendazole (TBZ), imazalil (IMZ), and pyrimethanil (PYR). However, their continued application results in the emergence of resistant pathogenic strains [5,6] and serious risks to human health and the environment [7]. Thus, there is an increasing interest in searching for new strategies to control phytopathogens [8,9] in all fresh fruit-producing areas.

Nowadays, the use of nanoparticles (NPs) has appeared as a promising tool to apply in diverse fields as medicine, electronics, energy, and agriculture [10]. However, the use of nanotechnology in the agricultural sector has raised concerns about its potential

environmental and health risks [11,12]. Nanoparticles (10–100 nm, in one dimension at least) could be synthesized by different processes, including physical, chemical, and biological methods [13], and offer significant advantages, particularly as antimicrobial agents. One of them includes a high surface-to-volume ratio that enhances interaction with the microorganisms [14]. Several reports have demonstrated the antimicrobial action of NPs containing metal ions such as zinc, silver, and copper [15–18]. In this regard, the action of ZnO-, CuO- and Ag-NPs against several fungi that affect diverse crops, such as *Fusarium solani*, *Botrytis cinerea*, *Alternaria alternata*, *Monilinia fructicola*, *Colletotrichum gloeosporioides*, *F. oxysporum*, and *Verticillium dahliae* [19,20], has been reported. Even though the antifungal effect of selenium-containing nanocomposites on citrus pathogens such as *Penicillium digitatum* has been recently studied [21,22], the use of metallic NPs on these phytopathogens has not been explored. Therefore, the aims of this study were to synthesize the NPs of ZnO, CuO, and Ag and to evaluate their antifungal action against local isolates such as *G. citri-aurantii* and both fungicide-sensitive and -resistant *Penicillium* spp.

2. Materials and Methods

2.1. Chemicals

ZnC₄H₆O₄ (Bernangel, Buenos Aires, Argentina); NaOH, Isopropanol, Ethylene Glycol (EG), and H₂O₂ (Cicarelli, Santa Fe, Argentina); CuSO₄, AgNO₃ (Anedra de Research Ag, Buenos Aires, Argentina); KOH (Merck, Darmstadt, Germany); Polyvinylpyrrolidone (PVP K30), Tween 80, and Dichlorofluorescein diacetate (H₂DCFDA) (Sigma-Aldrich, Chemical Co., St. Louis, MO, USA); SYTOX™ Green nucleic acid stain (Thermo Fisher Scientific Inc., Waltham, MA, USA). Other chemicals used were of analytical grade.

2.2. Synthesis of Zinc Oxide Nanoparticles

For the synthesis of ZnO-NPs, the protocol reported by Sandoval et al. [23] was followed. This process involves a low-temperature reaction (ice bath) using 230 mL of 0.0012 M zinc acetate and 20 mL of 0.02 M NaOH, both in isopropanol. Subsequently, this mix was heated to 65 °C for 2 h, resulting in the formation of a transparent suspension of NPs. Finally, isopropanol was removed through evaporation at 65 °C under a vacuum pressure of 400 mmHg to obtain fine powder. Different concentration suspensions were prepared by resuspending the powder in isopropanol.

2.3. Synthesis of Cupric Oxide Nanoparticles

A green synthesis approach was carried out for the preparation of CuO-NPs [24], using Aloe Vera (AV) extract. Five leaves were cleaned with distilled water, fragmented into small pieces, and dried in an oven set at 80 °C for 24 h. To obtain AV extract, 10 g of dried material was pulverized using a pestle, resuspended in 100 mL water, and boiled for 20 min. For the synthesis of CuO-NPs, 10 mL of 0.3 M CuSO₄ reacted with 50 mL of 10% AV extract at 100 °C for 1 h, with the formation of a black precipitate. Subsequently, the product was dried in an oven at 80 °C and underwent a sintering procedure at 300 °C for 30 min in muffle to improve size and form. The resulting NPs were maintained in darkness. To prepare the work suspension, CuO-NPs were resuspended in water and sonicated to obtain a dispersed suspension.

2.4. Synthesis of Silver Nanoparticles

Silver nanoparticles were synthesized according to Leng et al. [25] with some modification, using polyvinylpyrrolidone as a stabilizer. In a typical synthesis procedure, 35 mL of ethylene glycol (EG) was heated to 160 °C at agitation speed of 800 rpm. Then, 15 mL of EG containing 0.65 M silver nitrate and 1.6 g polyvinylpyrrolidone was gradually added to the stirring solution, maintaining an addition rate of 1 mL min⁻¹. Upon completion of the reduction reaction, the resulting mixture was cooled to room temperature. Finally, the Ag-NPs were separated from EG by a dilution process with distilled water and three rounds of centrifugation at 15,800 × g for 20 min each to obtain a Ag-NPs suspension in water.

2.5. Characterization of Metallic Nanoparticles

The ZnO-, CuO- and Ag-NPs obtained were characterized by UV-visible spectroscopy (Beckman DU7500 UV-VIS Diode array spectrometer, Spectralab Scientific Inc., Markham, ON, Canada). The form and size were determined using transmission electron microscopy (TEM) (Zeiss-Leo 906E, Zeiss, Oberkochen, Germany) and scanning electron microscopy (SEM) (Zeiss-Supra 55VP, Zeiss, Oberkochen, Germany). Elemental composition of NPs was determined using energy-dispersive spectroscopy (EDS), with an Inca Penta FET X3 instrument, Oxford (CIME-CONICET-UNT, Tucumán, Argentina), and X-ray diffraction (XRD), performed using an X-ray diffractometer (Rigaku Miniflex 300, Rigaku, Tokyo, Japan) operated at 30 kV and 100 mA, utilizing CuK α radiation with a wavelength of 1.5406 Å within the 2 θ angle range of 20° to 80°. The hydrodynamic diameter of NPs was determined using dynamic light scattering (DLS) and the Zeta potential (ξ) value was determined using a Horiba SZ-100 analyzer (Horiba Ltd., Kyoto, Japan). DLS measurements were conducted at a detection angle of 173°, and 100 fixed runs were performed for each sample, with a duration of 30 s per run. Data analysis was performed on Horiba NextGen Project SZ-100 (P2000447001J 2.00) to obtain the hydrodynamic radius and charges of the NPs.

2.6. Fungal Isolates and Conidial Suspensions Preparation

For the evaluations of lemon phytopathogens, fungal isolates previously characterized from the INSIBIO (CONICET-UNT) laboratory collection were used. These included fungicide-sensitive variants of *P. digitatum* (PDS, F-Pd07-S) and *P. italicum* (PIS, F-Pi09-S), and fungicide-resistant variants to imazalil, thiabendazole, and pyrimethanil from *P. digitatum* (PDR, F-Pd17-R31) and *P. italicum* (PIR, F-Pi15-R29) [26]. Additionally, a *G. citri-aurantii* (GC, F-Gc-S) isolate was included. For the preparation of the conidial suspension, the fungi were allowed to grow on potato dextrose agar (PDA) for 5 d at 22 \pm 1 °C. Sterile distilled water containing 0.05% Tween 80 (Sigma-Aldrich) was used to scrape the colony surface, and the conidia were collected and filtered through two layers of cheesecloth to remove hyphal fragments. The cellular concentration was adjusted with water to 1 \times 10⁶ conidia mL⁻¹ following counting in a Neubauer chamber [27].

2.7. Fruit

Lemons (*Citrus limon* (L.) Burm. F., cv. Eureka) were harvested at Las Tipas farm (Citrus Fruits S.R.L) from Tucumán, Argentina (26°37'60.0" S 65°25'00.0" W) and were free from any postharvest treatment or coating. Before treatments, each lemon was superficially disinfected (70% ethanol), rinsed with tap water, and allowed to air-dry at room temperature.

2.8. Determination of Conidia Growth and Minimum Fungicidal Concentration

Different approaches were used to assess the antifungal effect of NPs against the phytopathogenic isolates. In the case of ZnO-NPs, a test in potato dextrose liquid medium was conducted, covering a concentration range of up to 5000 μ g mL⁻¹. The effect of CuO-NPs and Ag was first assessed through a semiquantitative assay. This analysis was conducted by exposing conidial suspensions to different concentrations of CuO-NPs (from 100 to 1000 μ g mL⁻¹) and Ag-NPs (from 1 to 10 μ g mL⁻¹) for 24 h. Subsequently, a 5 μ L aliquot of treated suspensions was spotted onto PDA medium using serial dilutions (undiluted, 1/100, and 1/1000). On the other hand, viability was quantified in terms of colony-forming units per milliliter (CFU mL⁻¹) after exposure of the conidia to different concentrations of CuO-NPs or Ag for 24 h. Colonies were counted after 4 d of incubation at 22 \pm 1 °C. The minimum fungicidal concentration (MFC) is defined as the lowest concentration of NPs resulting in the death of 99.9% of the inoculum [28].

2.9. Determination of Infective Capacity of Treated Conidia

To assess the residual infectivity on the conidia of lemons after treatment with the NPs, a method described by Cerioni et al. [27] was followed, with some modifications. The artificial inoculation was performed using a steel rod previously immersed in control or treated conidial suspensions by exposing conidia to different concentrations of CuO- or Ag-NPs for 24 h. The rod tip was 1 mm wide and 2 mm long, which penetrated both flavedo and albedo tissues but not juice sacs of lemons. Fruit was stored at 20 °C and 95% relative humidity for 5 d, and incidence of infection was recorded at inoculation sites. The asymptomatic fruit was stored for 14 d before being discharged.

2.10. Evaluation of Conidial Membrane Integrity

To determine the impact of NPs on conidial membrane integrity, the fluorescent probe SYTOX™ Green (Thermo Fisher, Buenos Aires, Argentina) was used, following the protocol described by Olmedo et al. [29]. Conidial suspensions were treated at MFC or sublethal concentration for each NP for 24 h and then were washed and incubated with SYTOX™ Green (5 µM) for 30 min in darkness. Conidia were visualized under a fluorescence microscope Olympus IX51 equipped with an Olympus digital camera, QColor5 (Q-imaging). The fluorescence emission was examined and photographed using a filter set of 450–490 nm for excitation and 515–565 nm for emission. Three replicates were performed for each condition, and the assay was repeated three times.

2.11. Quantification of Reactive Oxygen Species Accumulation on Conidia

To determine the accumulation of reactive oxygen species (ROS) after treatments with NPs, a protocol reported by Cerioni et al. [30] was followed, with some modifications. Conidial suspensions were treated as described above, washed, and incubated with 10 µM H₂DCFDA probe in darkness overnight. After removing the probe, the fluorescence intensity was measured using an ISS-PCI spectrofluorometer (Champaign, IL, USA) and normalized with respect to the initial conidia concentration. Conidia treated with 600 mM H₂O₂ was included as positive control of ROS formation.

2.12. Evaluation of Conidia Ultrastructure

Conidia treated for 24 h with metallic NPs at the MFC or water (controls) were ultrastructural characterized through transmission electron microscopy (TEM). Conidia were processed as described by Cerioni et al. [30]. Observations were made using a Hitachi HT7800 (Hitachi, Chiyoda City, Japan) transmission electron microscope, available at the Comprehensive Center for Electron Microscopy (CME, CONICET-UNC, Córdoba, Argentina).

2.13. Application of Ag-NPs on Lemons

The Ag-NPs were evaluated by in situ application on lemons wounded using a stainless steel rod previously immersed into a freshly prepared conidial suspension of *P. digitatum* (PDS and PDR). After inoculation, the lemons were allowed to dry for 30 min at room temperature. Subsequently, 10 µL of Ag-NPs at concentrations of 500 and 1000 µg mL⁻¹ were directly applied to the wounds. As a control, 10 µL of water was added to the wounds. The lemons were incubated for 5 d in a chamber with controlled conditions of temperature (20 °C) and relative humidity (95%). The results were obtained by evaluating the incidence of the disease.

2.14. Statistical Analysis

For the in vitro assays, three complete sets of experiments were conducted, encompassing three repetitions for each condition. The in vivo assays comprised two repetitions involving 10 lemons (each with two wounds) for each condition. In all cases, the data underwent variance analysis, followed by Tukey's test using Infostat software v 2020I [31]. Differences of $p \leq 0.05$ were considered significant.

3. Results

3.1. Synthesis and Characterization of Nanoparticles

Three types of metallic NPs (ZnO-, CuO-, and Ag-NPs) were synthesized, following methods described in the Materials and Methods section, and were subjected to characterization through various analytical techniques, as shown in Figure 1. The analysis involved UV-VIS spectroscopy from 230 to 600 nm of the NP preparations resuspended on the solvents used for subsequent *in vitro* evaluation, either isopropanol for ZnO-NPs or water for the other NPs (Figure 1a). In the case of ZnO-NPs, the spectrum exhibited absorption from wavelengths in the UV range up to nearly 360 nm, followed by a sharp decrease in the absorbance. For CuO-NPs, an absorbance peak was observed at 310 nm, while in the case of Ag-NPs, a surface plasmon resonance signal was detected at 406 nm. As a reference to the baseline, the spectra of solvents were included. An X-ray powder diffraction analysis was carried out to obtain information on the elemental composition of the NPs (Figure 1b). In the case of ZnO-NPs, precise correlations were found with the Bragg planes (100), (101), (002), (102), (110), (103), (200), (112), and (201). For CuO-NPs, the following peaks were identified: (110), (002), (111), (111), (200), (202), (202), (112), (022), and (311). The X-ray diffraction pattern for the Ag-NPs presented peaks at (111), (200), and (220). Thus, distinctive diffraction peaks were observed for each type of NP, corresponding to a precise correlation between the peaks and their respective materials. Furthermore, the composition of the NPs was confirmed by energy-dispersive X-ray spectroscopy (EDS) (Figure 1c). For ZnO-NPs, significant proportions of O₂ (22.15%) and Zn (20.83%) were identified, confirming the ZnO nature of the NP. The EDS analysis of CuO-NPs revealed that Cu (73.89%) and O₂ (23.32%) were the predominant elements, unequivocally demonstrating the CuO nature of the sample. The elemental composition of the Ag-NPs revealed a Ag content of 73.53%, confirming its metallic nature, with a significant presence of C (17.67%) attributed to the stabilizer (PVP). NP morphology was assessed using scanning electron and transmission electron microscopies (SEM and TEM) (Figures 1d and 1e, respectively), with most NPs displaying spherical shapes. TEM also provided the calculated NP average sizes: 11 ± 0.6 nm for ZnO-NPs, 11 ± 0.5 nm for CuO-NPs, and 25 ± 2.6 nm for Ag-NPs. Additionally, a dynamic light scattering (DLS) analysis was performed to assess the surface charge and to determine the hydrodynamic radius of the NPs. The zeta potential values for the NPs were 20.0 mV for ZnO-NPs, -39.8 mV for CuO-NPs, and -41.8 mV for Ag-NPs. The hydrodynamic radius of ZnO-NPs was not determined due to the presence of the organic solvent, while CuO-NPs and Ag-NPs show hydrodynamic radii of approximately 9 nm and 82 nm, respectively.

3.2. Antifungal Action of Nanoparticles

The antifungal activity of metallic NPs against the fungicide-sensitive or -resistant phytopathogens was evaluated. ZnO-NPs did not present antifungal activity at analyzed concentrations up to $5000 \mu\text{g mL}^{-1}$. Figure 2 shows a semiquantitative assessment of conidial growth after 24-h exposure to CuO- or Ag-NPs. In control samples, characteristic colonies for each pathogen were observed whose radial growth decreased as the conidial dilution increased, as expected. The colony growth of all pathogens was inhibited when conidia were pre-treated with a concentration of $1000 \mu\text{g mL}^{-1}$ for NPs-CuO and at $10 \mu\text{g mL}^{-1}$ for NPs-Ag. At concentrations that are 10-fold lower, a decrease in radial growth compared to untreated controls was observed, indicating sublethal conditions in which only part of the conidia remained viable. Therefore, colony-forming units per milliliter (CFU mL⁻¹) were determined for quantification (Table 1). At a sublethal concentration of $100 \mu\text{g mL}^{-1}$ of CuO-NPs, a 62% inhibition was observed in the PDS population, which represents a decrease in an order of magnitude in the values of CFU mL⁻¹, from 1.1×10^6 to 2.0×10^5 . Additionally, an 84% inhibition was observed for PDR, with a decrease to 9.5×10^4 CFU mL⁻¹. The viability inhibition for PIS, PIR, and GC isolates was close to 90%. For Ag-NPs, at a sublethal concentration ($1 \mu\text{g mL}^{-1}$), the range of inhibition varied between 95 and 99% for all the evaluated fungi, except for PDR with a 75% reduction

in conidia viability. The minimum fungicide concentration (MFC) was 1000 $\mu\text{g mL}^{-1}$ for CuO-NPs and 10 $\mu\text{g mL}^{-1}$ for Ag-NPs for all phytopathogens evaluated.

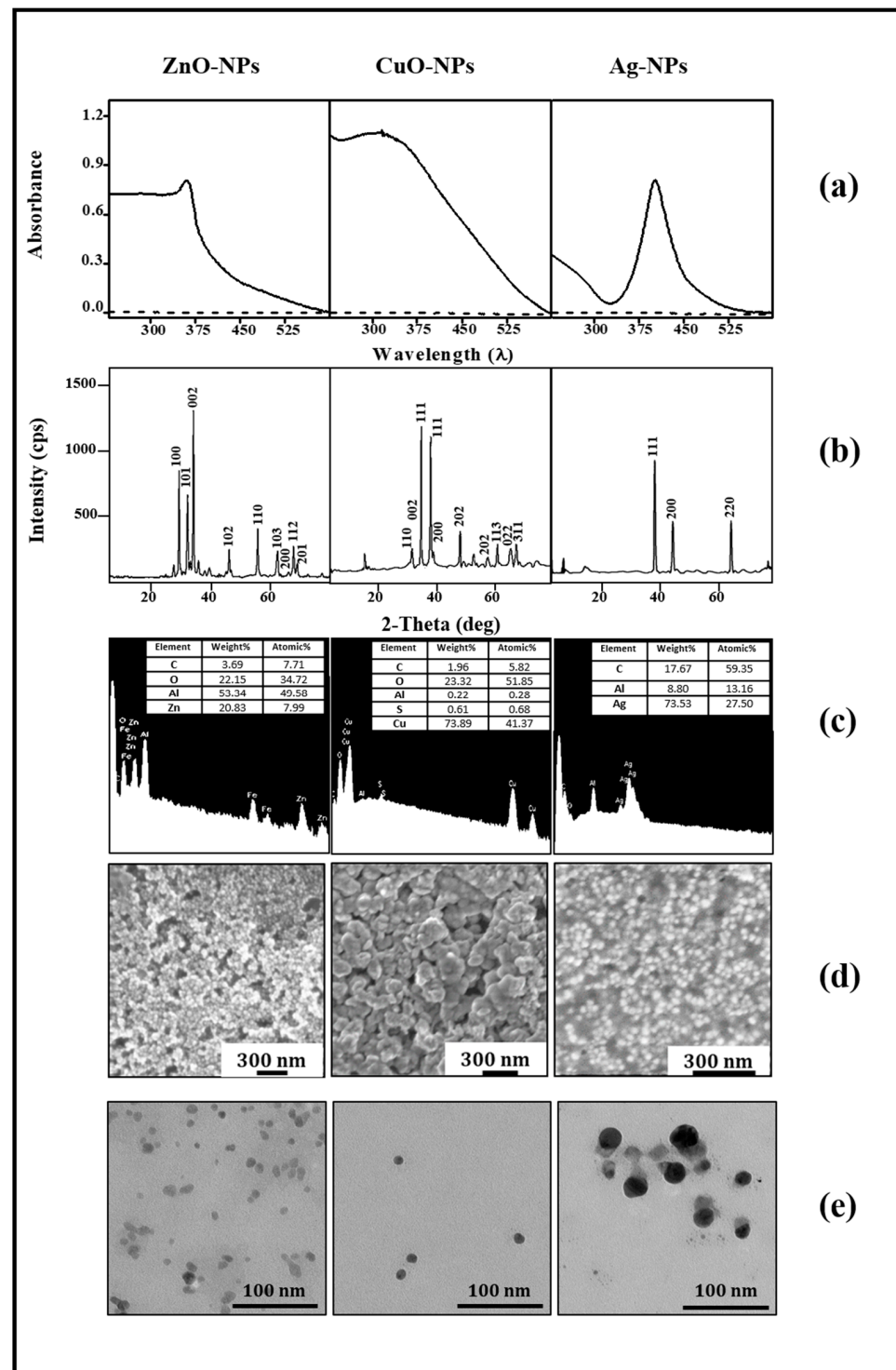


Figure 1. Characterization of nanoparticles by spectroscopic techniques and electron microscopy. (a) UV-VIS spectra of NPs resuspended in isopropanol (ZnO-NPs) or water (CuO- and AgNPs) (solid line), and solvent reference baseline (dotted line); (b) X-ray spectra (XRD); (c) energy-dispersive spectra (EDS); (d) scanning electron microscopy (SEM); (e) transmission electron microscopy (TEM). As indicated, the left panels show ZnO-NPs, the central panels CuO-NPs, and the right panels Ag-NPs. Bars in the electron microscopy images indicate the scale.

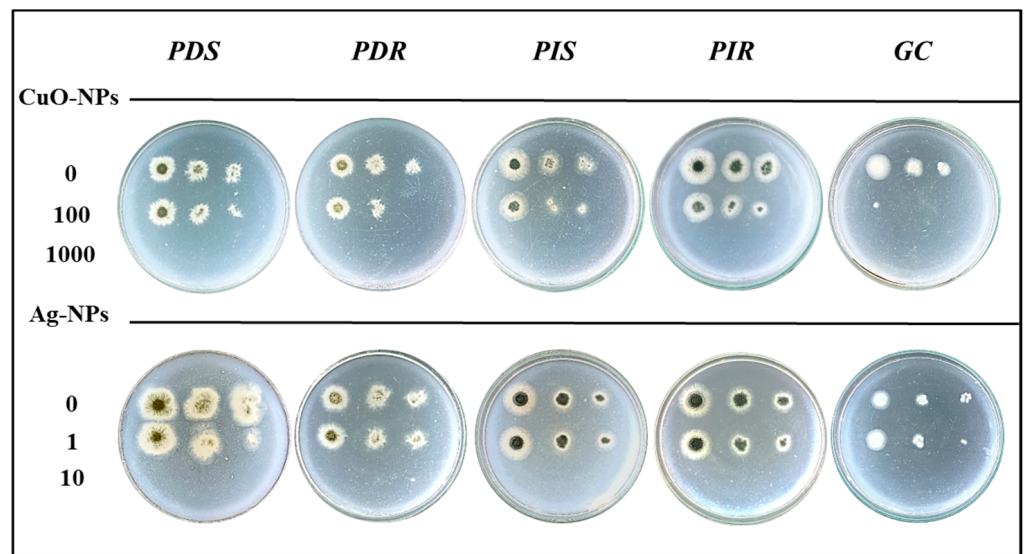


Figure 2. Antifungal activity of nanoparticles. Conidial suspensions (10^6 CFU mL⁻¹) of the indicated isolates were exposed for 24 h to different NP concentrations ($\mu\text{g mL}^{-1}$). After treatments, serial dilutions of the cells were plated on PDA and grown for 4 d at 22 ± 1 °C. Controls corresponding to cells incubated without NPs were included. The growth of conidia treated with CuO-NPs (**upper panel**) and Ag-NPs (**lower panel**) is shown as representative images from three independent experiments. The last point of each row contains a 1/1000 dilution of the original culture.

Table 1. Effect of nanoparticles on phytopathogens conidia viability*.

Pathogens	Control	CuO-NPs ($\mu\text{g mL}^{-1}$)		Ag-NPs ($\mu\text{g mL}^{-1}$)	
	-	100	1000	1	10
CFU mL ⁻¹					
PDS	1.1×10^6 a	2.0×10^5 b	6.5×10^1 c	2.2×10^4 b	0 b
PDR	9.0×10^5 a	9.5×10^4 b	9.6×10^1 c	1.5×10^5 b	0 b
PIS	9.5×10^5 a	4.8×10^4 b	1.7×10^1 c	1.7×10^4 b	0 b
PIR	1.2×10^6 a	2.5×10^4 b	1.0×10^1 b	4.0×10^3 b	0 b
GC	8.5×10^5 a	1.0×10^2 b	0 b	5.0×10^3 b	0 b

* Conidial suspensions were exposed to NPs both at sublethal concentrations and MFC, as indicated. Samples treated only with water were used as controls. Different letters indicate significant differences comparing each pathogen to their respective control according to Tukey’s analysis with a p -value ≤ 0.01 . PDS-, PDR-, PIS-, and PIR-sensitive and -resistant *P. digitatum* and *P. italicum*; GC: *G. citri-aurantii*.

3.3. Residual Infection of Conidia Treated with Nanoparticles

The residual infectivity of conidia treated for a 24 h period with CuO- and Ag-NPs was evaluated on Eureka lemons (Figure 3a,b). All the fruit inoculated with untreated conidia exhibited high disease incidence at 5 d of incubation. When conidia were treated with CuO-NPs at a sublethal concentration ($100 \mu\text{g mL}^{-1}$), PDS, PDR, and PIS registered a similar incidence to controls, while a reduction of nearly 70% was achieved for GC, being the most sensitive of the tested fungi. On the other hand, when conidia were treated with Ag-NPs at a sublethal concentration ($1 \mu\text{g mL}^{-1}$), a significant decrease in disease incidence was achieved for all the pathogens, with inhibitions between 70 and 95%. As was expected, when the conidia were treated either with CuO-NPs or Ag-NPs at the MFC, no development of the postharvest diseases was observed until 14 d incubation.

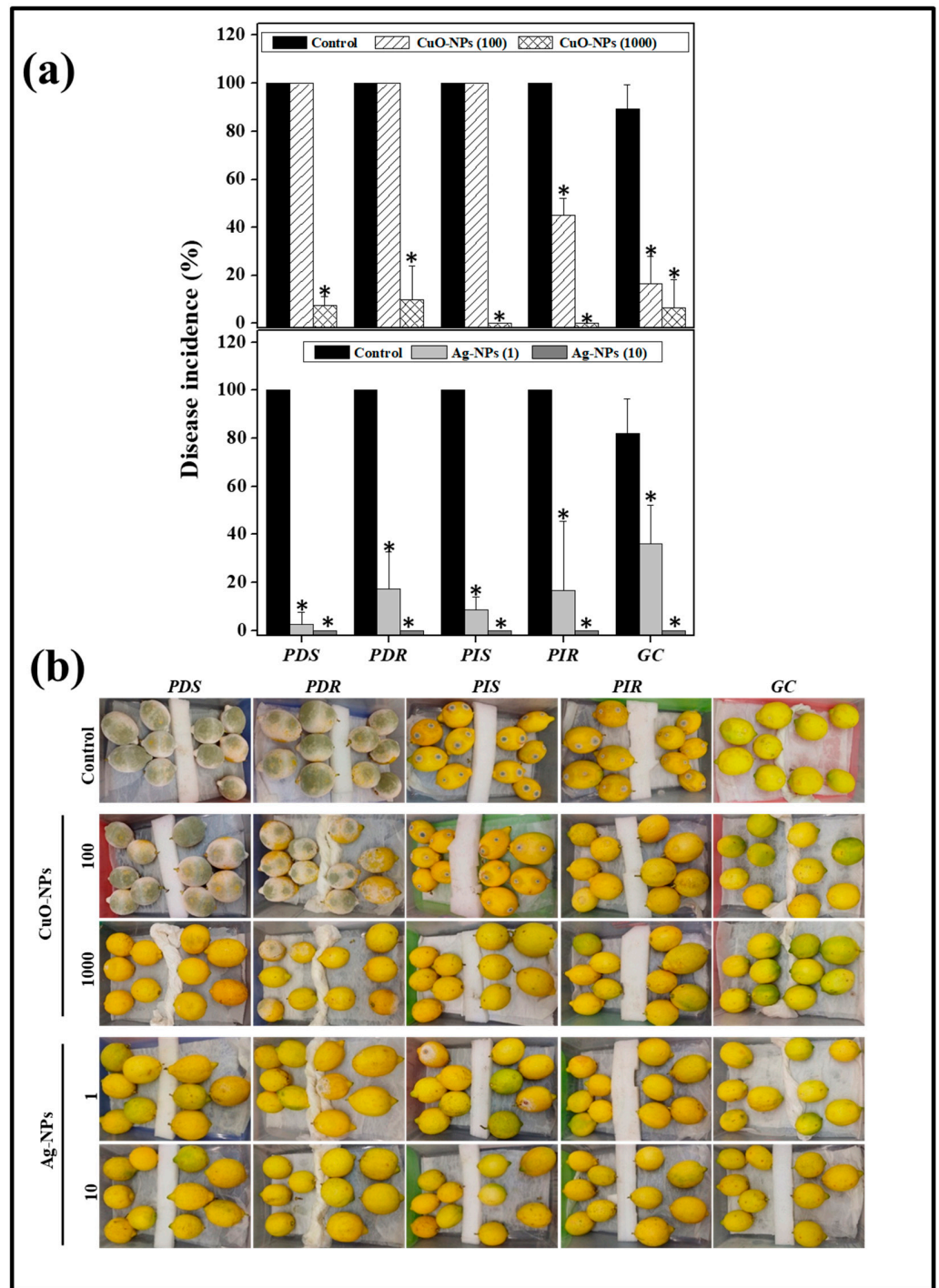


Figure 3. Effect of nanoparticles on infectivity capacity of conidia on lemons. (a) Lemons were inoculated using conidia treated with the indicated NP concentrations ($\mu\text{g mL}^{-1}$) and the incidence of the disease was evaluated as a percentage of the corresponding control. The results were averaged from two experiments, using 10 lemons and 2 wounds in each case. Asterisks (*) indicate significant differences with respect to the control group according to Tukey’s analysis, with a p -value ≤ 0.05 (b) Representative images of disease incidence for the specified isolate and conditions.

3.4. Effect on Conidial Membrane Integrity After Nanoparticle Treatments

In order to analyze the effect of NPs on fungal conidia, a study of the cell membrane integrity was carried out using the SYTOXTM Green probe (Figure 4). In the dark field, fluorescent conidia were observed for all fungal isolates treated in the presence of CuO-

and Ag-NPs, indicating increases in membrane permeability in a concentration-dependent manner. As the positive control of membrane damage, a treatment with 600 mM H₂O₂ was included, which shows fluorescence for all the phytopathogens, similar to NP treatments. No fluorescence emission was observed in samples incubated with water. It should be noted that most of the conidia were clearly visible in the bright field, except at the maximum CuO-NP concentration due to dark sediment being present.

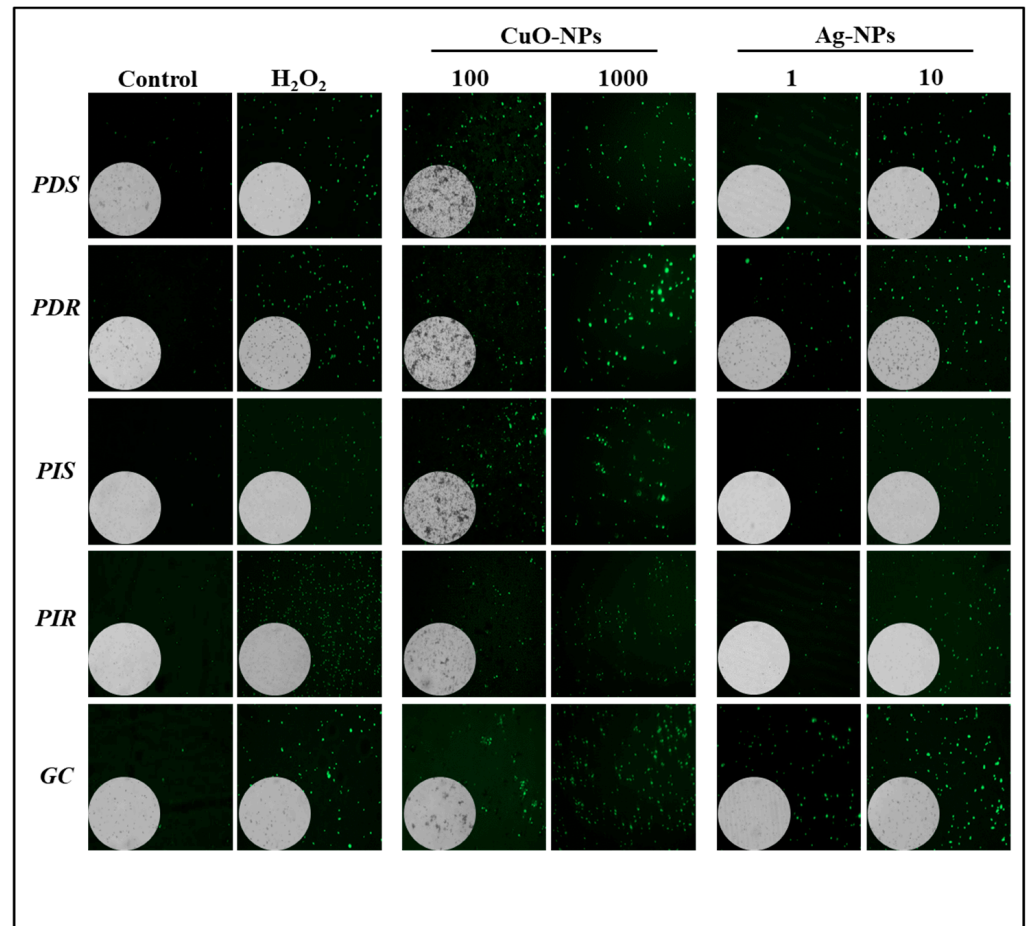


Figure 4. Effect of nanoparticles on membrane integrity. Conidial suspensions of indicated isolates were treated for 24 h with the indicated concentration of NPs ($\mu\text{g mL}^{-1}$) and then exposed to 0.5 μM SYTOXTM Green for 30 min. Fluorescent field images at a 40 \times magnification accompanied by a bright field (insets) are shown. The left panels display negative and positive controls, corresponding to conidia treated either with water or 600 mM H₂O₂, respectively. The images are representative of three independent experiments.

3.5. Production of Reactive Oxygen Species After Nanoparticle Treatments

A proposed mechanism for the action of NPs on microorganisms is the induction of ROS generation. Figure 5 shows the quantitative evaluation of ROS accumulation in treated conidia using the H₂DCFDA probe. At lethal and sublethal concentrations of CuO-NPs, a significant increase in ROS accumulation in the conidia was observed, with respect to the control, being 10-fold higher at the lethal concentration. Nevertheless, ROS production was not detected after 24 h of treatment with both Ag-NP concentrations in any of the evaluated pathogens.

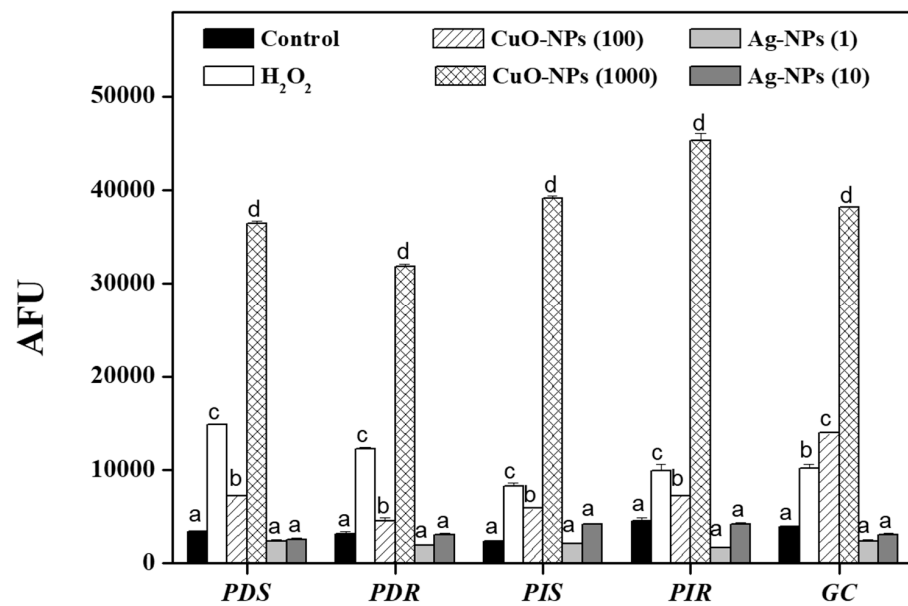


Figure 5. Effect of nanoparticles on ROS generation. After exposing conidia to the indicated concentrations of CuO- and Ag-NPs ($\mu\text{g mL}^{-1}$) for 24 h, the amount of intracellular ROS was determined. The results are expressed as the mean \pm standard deviation from three independent experiments. Different letters indicate significant differences between treatments according to Tukey’s analysis, with a p -value ≤ 0.05 .

3.6. Conidial Internal Structure After Nanoparticle Treatments

The ultrastructure of the conidia was examined using transmission electron microscopy (TEM) (Figure 6). All evaluated fungi in control condition revealed an appropriate organization of the cell walls and the cytoplasm and the presence of some internal structures as lipid bodies, indicating an overall undisturbed structure.

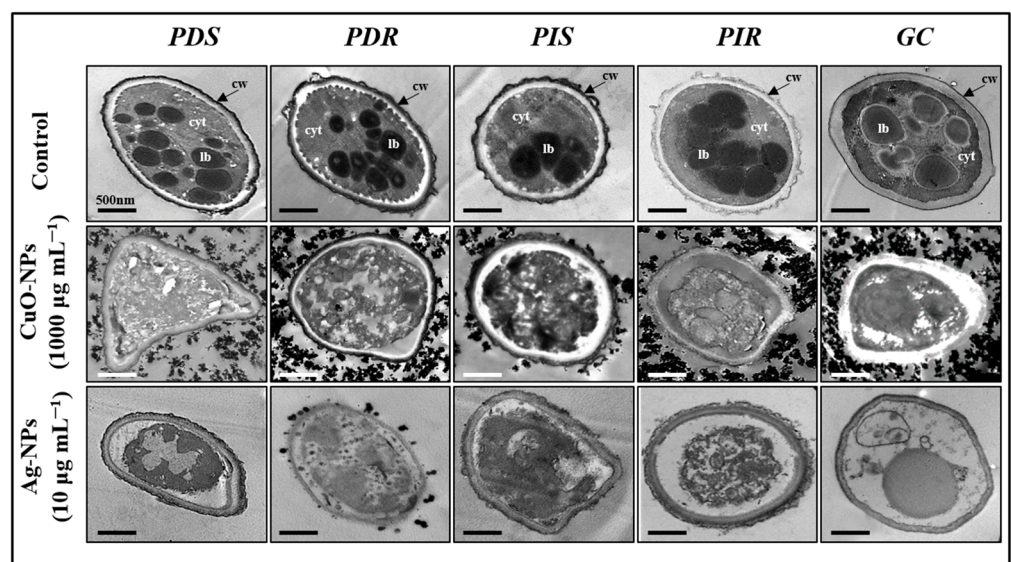


Figure 6. Intracellular damage induced by nanoparticles. Conidial suspensions were exposed to the minimum fungicidal concentration of NPs for 24 h and then visualized by transmission electron microscopy (TEM). The tests were repeated three times for each treatment, and at least two replicates were examined. The top panels show control conditions for each isolate, while the remaining panels display conidia treated with the indicated nanoparticles. In micrographs, a scale bar of 500 nm is represented. cw, cell wall; cyt, cytoplasm; lb, lipid body.

However, after exposing the conidia to the NPs at the MFC for 24 h, notable cellular damage was evident, including cell deformation and clear cytoplasmic disorganization, with the presence of intracellular cavities and vesicles. Significant modifications in the membrane and cell wall structure occurred, characterized by contraction and irregularities. Taken together, these results indicate irreversible cellular damage after treatment with both NPs.

3.7. Green Mold Incidence After In Situ Application of Ag-NPs on Lemons

Considering the higher in vitro efficacy of silver NPs against the tested fungi compared to the other NPs, the antifungal action of Ag-NPs was evaluated in situ on artificially inoculated lemons. In the control group, an elevated disease incidence was observed (around 90%) on inoculated fruit (Figure 7a,b). As expected, the application of IMZ at 500 µg mL⁻¹ showed differential results depending on the assayed fungal isolate. Indeed, IMZ was able to control green mold caused by fungicide-sensitive isolate, while it allowed a disease incidence nearly 65% for the resistant isolate. In contrast, the application of Ag-NPs demonstrated significant antifungal action against both *P. digitatum* isolates, presenting disease incidences below 10%.

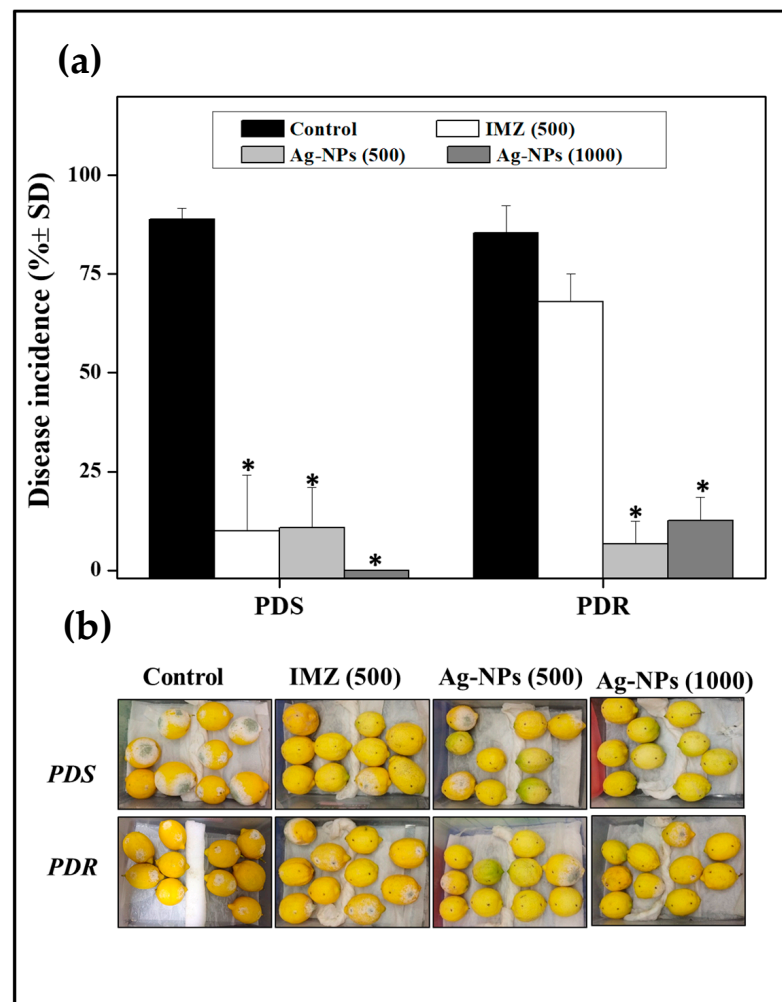


Figure 7. Disease incidence of green mold caused by sensitive and resistant strains. (a). The fruits were inoculated with a suspension of 1×10^5 CFU mL⁻¹ of the indicated strains and treated with 10 µL of NP suspensions at the indicated concentration, imazalil (commercial fungicide), or water (control). Green mold incidence was assessed as a percentage. Asterisks (*) indicate significant differences compared to the control group according to Tukey’s test, with a *p*-value ≤ 0.05. (b). Representative images of the treatment with Ag-NPs are shown.

4. Discussion

In this study, zinc oxide, cupric oxide, and silver NPs were synthesized, characterized, and applied to inhibit the growth of fungicide-sensitive or -resistant citrus phytopathogens, both in vitro and on the lemon fruit.

In all cases, the synthesized metallic NPs presented characteristic UV-VIS spectra, containing absorbance peaks that were consistent with those previously reported in the literature for each NP [25,32,33]. The nature and elemental composition of them were confirmed by XRD and EDS techniques. In addition, considering previous analyses [34,35] and the obtained zeta potential values, it was expected that CuO and Ag-NPs would present greater dispersion and stability in the colloidal suspension than those of ZnO-NPs. The average size of CuO-NPs, after the sintering process that eliminated all organic material, was similar according to DLS and TEM determinations. However, only the size measured by TEM was taken into account for Ag-NPs, since the DLS values might be overestimated by the PVP organic layer and the surrounding aqueous solvation layer, as previously argued [36]. The present characterization indicated that the obtained NPs exhibit two important features: nanometric size and spherical shape. The spherical shape facilitates a uniform distribution of the NPs, preventing the formation of aggregates and maximizing their contact area with microorganisms [32,37]. Furthermore, nanometric particles, bearing a higher surface-to-volume ratio, tend to display high antimicrobial activity due to the increased interaction with the microbial cell envelopes [25].

The present results demonstrated that CuO- and Ag-NPs exhibited antifungal activity against all evaluated fungi, whereas ZnO-NPs did not show activity. It is possible that the zeta potential value of ZnO-NPs affects suspension stability, leading to the NP aggregation in the incubation medium. The inhibition of all pathogens was achieved at a concentration of $10 \mu\text{g mL}^{-1}$ Ag-NPs, while a 100 times larger concentration of CuO-NPs was required to obtain a similar deleterious effect. At present, there are few reports where NPs were evaluated against filamentous fungi. Previous reports have demonstrated similar results when comparing different NPs against *Alternaria alternata* and *Pyricularia oryzae*, where Ag- and CuO-NPs were effective, while ZnO-NPs did not significantly inhibit mycelial growth compared to the control [38]. Malandrakis et al. [20] have evaluated the sensitivity of several fungi to both CuO- and Ag-NPs, showing a moderate inhibition only against *B. cinerea* at $307 \mu\text{g mL}^{-1}$ Ag-NPs. In another report, $150 \mu\text{g mL}^{-1}$ Ag-NPs were able to inhibit nearly 50% of the *P. verrucosum* population [39]. Note that in these reports, the Ag-NP concentration necessary to achieve the inhibitory effect was between 15- and 30-fold higher than that used in our conditions. In addition, Shammout and Awwad [40] reported *Aspergillus niger* growth inhibition using $5000 \mu\text{g mL}^{-1}$ CuO-NPs, showing more tolerance with respect to the phytopathogenic fungi tested here. It is worth noting that the effect of NPs against fungicide-sensitive and -resistant isolates was comparable, which could allow the control of postharvest diseases caused by fungal-resistant isolates.

When comparing the conidial infective capacity on lemons using treated fungi, Ag-NPs were more effective than CuO-NPs in reducing the residual incidence, impairing the progress of diseases even at a sublethal concentration. In that condition ($1 \mu\text{g mL}^{-1}$ of Ag-NPs), a decrease of nearly 96% in disease incidence was observed, although the colony-forming units (CFUs) counted (e.g., 10^4 CFU mL^{-1} for PDS) provided enough inoculum for mold development on lemons, as it has been previously reported [41,42].

The CuO-NPs and Ag-NPs induced cell disorganization and membrane permeability on the evaluated phytopathogens. The mechanisms of action of NPs on bacteria involve multiple cellular targets [37,43]. The use of treatments that affect multiple targets could reduce fungal development, in contrast to fungicides with a single mode of action, such as imazalil, which are often evaded by resistant isolates [44,45]. Additionally, CuO-NPs caused an increase in the generation of ROS, similar to what has been reported for the oomycete *Phytophthora nicotianae* by Chen et al. [46]. Ag-NPs (average size 25 nm) at the evaluated concentrations did not lead to ROS production after 24 h of treatment. The difference in ROS production between Ag-NPs and CuO-NPs may be attributed to a variety

of factors, such as size, concentration, chemical composition, and their interaction with the specific microorganisms. Despite this, it has been reported that Ag-NPs conduced to ROS accumulation in *Candida albicans* and *Fusarium graminearum* [47,48], supporting the present results. Carlson et al. [49] highlight the variability in ROS generation depending on nanoparticle size when acting over macrophages. They reported that 15 nm Ag-NPs generated ROS, while 30 nm particles did not, although both yielded positive results in cytotoxicity assays. Together, Ag-NPs cause severe ultrastructural damage and a strong inhibition of growth to all the citrus pathogens in the assayed conditions, despite the absence of ROS production.

Due to the best antifungal activity demonstrated to Ag-NPs, their efficacy to control green mold incidence was evaluated. This step was crucial to determine if the antifungal properties observed in vitro were maintained under conditions closer to practical applications. The obtained results show that the in situ application of 500 $\mu\text{g mL}^{-1}$ Ag-NPs was effective in decreasing the incidence of green mold on lemons, including mold caused by the *Penicillium* spp. fungicide-resistant isolate. Previous reports have explored the effect of several nanoparticles to control infectious diseases in fruits. Iliger et al. [50] used CuO-NPs to control rot in chili peppers caused by *Colletotrichum capsici* using 1000 $\mu\text{g mL}^{-1}$ of NPs. Saqib et al. [51] evaluated iron oxide nanoparticles in vivo on apricots infected with *Rhizopus stolonifer* and found that a concentration of 10,000 $\mu\text{g mL}^{-1}$ of NPs was needed to control this mold. It should be noted that metallic NPs can be risky for human health, since it is well known that may cause damaging effects, such as oxidative stress, cytotoxicity, and inflammation [52–54]. In this context, further research is necessary to assess the safety and viability of NPs (or their immobilized forms) before large-scale implementation for fruits, packaging, and commercial tanks.

5. Conclusions

In the present study, the antifungal activity of three types of NPs were evaluated providing a detailed description of their synthesis and characterization. CuO- and Ag-NPs presented the ability to inhibit in vitro lemon fungal pathogens. It has been observed that both NPs exert their action through membrane permeabilization and intracellular damage, while CuO-NPs also induced the production of ROS. Moreover, Ag-NPs reduced the residual infectivity of conidia even at sublethal concentrations and were able to control green mold on artificially inoculated lemons, especially mold caused by a fungicide-resistant isolate. Taken together, our results indicate that Ag-NPs are a promising alternative antifungal nanomaterial for the preservation of fruits against postharvest fungal pathogens.

Author Contributions: Conceptualization, L.C., S.I.V. and V.A.R.; Methodology, C.G.B., L.C., M.A.D., A.E.L., P.A. and S.I.V.; Validation, C.G.B.; Formal analysis, L.C., M.T., S.I.V. and V.A.R.; Investigation, C.G.B., L.C., M.T., S.I.V. and V.A.R.; Data curation, C.G.B., L.C., M.A.D., S.I.V. and V.A.R.; Writing—original draft, C.G.B., S.I.V. and V.A.R.; Writing—review & editing, C.G.B., L.C., M.A.D., A.E.L., P.A., M.T., S.I.V. and V.A.R.; Supervision, S.I.V. and V.A.R.; Funding acquisition, S.I.V. and V.A.R. All authors have read and agreed to the published version of the manuscript.

Funding: This work was supported by grants from Agencia Nacional de Promoción Científica y Tecnológica (PICT 2019-1380), CONICET (PIP 2547), and Universidad Nacional de Tucumán (PIUNT D750; PIUNT D768). CGB is a fellow from CONICET.

Data Availability Statement: The original contributions presented in the study are included in the article, further inquiries can be directed to the corresponding authors.

Acknowledgments: We extend our special thanks to Las Tipas farm for generously providing the lemons and to Cintia Romero for supplying silver nanoparticles standard suspension useful for quantitation. Additionally, we thank Fernando Dupuy and Jakeline Zuluaga-Acosta for their technical contributions. We also thank Carolina Navarro for her help in the X-ray analysis.

Conflicts of Interest: The authors declare that they have no conflict of interest.

References

- Eckert, J.W. Post-harvest diseases of citrus fruits. *Outlook Agric.* **1978**, *9*, 225–232. [CrossRef]
- Pitt, J.I.; Hocking, A.D. Primary Keys and Miscellaneous Fungi. In *Fungi and Food Spoilage*; Pitt, J.I., Hocking, A.D., Eds.; Springer: Berlin/Heidelberg, Germany, 2009.
- Wang, W.; Liu, S.; Deng, L.; Ming, J.; Yao, S.; Zeng, K. Control of Citrus Post-harvest Green Molds, Blue Molds, and Sour Rot by the Cecropin A-Melittin Hybrid Peptide BP21. *Front. Microbiol.* **2018**, *9*, 2455. [CrossRef]
- Federcitrus. The Argentine Citrus Industry. 2023. Available online: <http://www.federcitrus.org/estadisticas/> (accessed on 4 November 2024).
- Palou, L.; Ali, A.; Fallik, E.; Romanazzi, G. GRAS, plant- and animal-derived compounds as alternatives to conventional fungicides for the control of postharvest diseases of fresh horticultural produce. *Postharvest Biol. Technol.* **2016**, *122*, 41–52. [CrossRef]
- Sánchez-Torres, P.; Tuset, J.J. Molecular insights into fungicide resistance in sensitive and resistant *Penicillium digitatum* strains infecting citrus. *Postharvest Biol. Technol.* **2011**, *59*, 159–165. [CrossRef]
- Kinay, P.; Mansour, M.F.; Gabler, F.M.; Margosan, D.A.; Smilanick, J.L. Characterization of fungicide-resistant isolates of *Penicillium digitatum* collected in California. *Crop Prot.* **2007**, *26*, 647–656. [CrossRef]
- Elshafie, H.S.; Camele, I. An overview of the biological effects of some mediterranean essential oils on human health. *BioMed Res. Int.* **2017**, *2017*, 9268468. [CrossRef]
- Usall, J.; Ippolito, A.; Sisquella, M.; Neri, F. Physical treatments to control postharvest diseases of fresh fruits and vegetables. *Postharvest Biol. Technol.* **2016**, *122*, 30–40. [CrossRef]
- Sohail, M.I.; Waris, A.A.; Ayub, M.A.; Usman, M.; ur Rehman, M.Z.; Sabir, M.; Faiz, T. Environmental application of nanomaterials: A promise to sustainable future. *Compr. Anal. Chem.* **2019**, *87*, 1–54.
- Khot, L.R.; Sankaran, S.; Maja, J.M.; Ehsani, R.; Schuster, E.W. Applications of nanomaterials in agricultural production and crop protection: A review. *Crop Prot.* **2012**, *35*, 64–70. [CrossRef]
- Okeke, E.S.; Ezeorba, T.P.C.; Mao, G.; Chen, Y.; Feng, W.; Wu, X. Nano-enabled agrochemicals/materials: Potential human health impact, risk assessment, management strategies and future prospects. *Environ. Pollutio* **2022**, *295*, 118722. [CrossRef]
- Hall, J.B.; A Dobrovolskaia, M.; Patri, A.K.; E McNeil, S. Characterization of nanoparticles for therapeutics. *Nanomedicine* **2007**, *2*, 789–803. [CrossRef] [PubMed]
- Wang, L.; Hu, C.; Shao, L. The antimicrobial activity of nanoparticles: Present situation and prospects for the future. *Int. J. Nanomed.* **2017**, *12*, 1227–1249. [CrossRef] [PubMed]
- Alghuthaymi, M.A.; Almoammar, H.; Rai, M.; Said-Galiev, E.; Abd-Elsalam, K.A. Myconanoparticles: Synthesis and their role in phytopathogens management. *Biotechnol. Biotechnol. Equip.* **2015**, *29*, 221–236. [CrossRef] [PubMed]
- Dimkpa, C.O.; McLean, J.E.; Britt, D.W.; Anderson, A.J. Antifungal activity of ZnO nanoparticles and their interactive effect with a biocontrol bacterium on growth antagonism of the plant pathogen *Fusarium graminearum*. *Biometals* **2013**, *26*, 913–924. [CrossRef]
- He, L.; Liu, Y.; Mustapha, A.; Lin, M. Antifungal activity of zinc oxide nanoparticles against *Botrytis cinerea* and *Penicillium expansum*. *Microbiol. Res.* **2011**, *166*, 207–215. [CrossRef]
- Kim, J.; Lee, J.; Kwon, S.; Jeong, S. Preparation of biodegradable polymer/silver nanoparticles composite and its antibacterial efficacy. *J. Nanosci. Nanotechnol.* **2009**, *9*, 1098–1102. [CrossRef]
- Malandrakis, A.A.; Kavroulakis, N.; Avramidou, M.; Papadopoulou, K.K.; Tsaniklidis, G.; Chrysikopoulos, C.V. Metal nanoparticles: Phytotoxicity on tomato and effect on symbiosis with the *Fusarium solani* FsK strain. *Sci. Total Environ.* **2021**, *787*, 147606. [CrossRef]
- Malandrakis, A.A.; Kavroulakis, N.; Chrysikopoulos, C.V. Use of copper, silver and zinc nanoparticles against foliar and soil-borne plant pathogens. *Sci. Total Environ.* **2019**, *670*, 292–299. [CrossRef]
- Elshafie, H.S.; Osman, A.; El-Saber, M.M.; Camele, I.; Abbas, E. Antifungal Activity of Green and Chemically Synthesized ZnO Nanoparticles against *Alternaria citri*, the Causal Agent Citrus Black Rot. *Plant Pathol. J.* **2023**, *39*, 265–274. [CrossRef]
- Salem, M.F.; Abd-Elraoof, W.A.; Tayel, A.A.; Alzuair, F.M.; Abonama, O.M. Antifungal application of biosynthesized selenium nanoparticles with pomegranate peels and nanochitosan as edible coatings for citrus green mold protection. *J. Nanobiotechnology* **2022**, *20*, 182. [CrossRef]
- Sandoval, C.; Marin, O.; Real, S.; Comedi, D.; Tirado, M. Electrophoretic deposition of ZnO nanostructures: Au nanoclusters on Si substrates induce self-assembled nanowire growth. *Mater. Sci. Eng. B* **2014**, *187*, 21–25. [CrossRef]
- Ahmaruzzaman, M. Ecofriendly biosynthetic route for production of Cu nanoparticles and evaluation of their photocatalytic activities for degradation of organic compounds. *J. Iran. Chem. Soc.* **2022**, *19*, 645–654. [CrossRef]
- Leng, Z.; Wu, D.; Yang, Q.; Zeng, S.; Xia, W. Facile and one-step liquid phase synthesis of uniform silver nanoparticles reduction by ethylene glycol. *Optik* **2018**, *154*, 33–40. [CrossRef]
- Olmedo, G.M.; Debes, M.A.; Sepúlveda, M.; Ramallo, J.; A Rapisarda, V.; Cerioni, L.; Volentini, S.I. Overcoming lemon postharvest molds caused by *Penicillium* spp. multiresistant isolates by the application of potassium sorbate in aqueous and wax treatments. *J. Food Sci.* **2023**, *88*, 2960–2967. [CrossRef] [PubMed]
- Cerioni, L.; Rapisarda, V.A.; Hilal, M.; Prado, F.E.; Rodríguez-Montelongo, L. Synergistic antifungal activity of sodium hypochlorite, hydrogen peroxide, and cupric sulfate against *Penicillium digitatum*. *J. Food Prot.* **2009**, *72*, 1660–1665. [CrossRef]
- Kurita, N.; Miyaji, M.; Kurane, R.; Takahara, Y. Antifungal Activity of Components of Essential Oils. *Agric. Biol. Chem.* **1981**, *45*, 945–952.

29. Olmedo, G.M.; Cerioni, L.; González, M.M.; Cabrerizo, F.M.; Rapisarda, V.A.; Volentini, S.I. Antifungal activity of β -carboline on *Penicillium digitatum* and *Botrytis cinerea*. *Food Microbiol.* **2017**, *62*, 9–14. [CrossRef]
30. Cerioni, L.; Volentini, S.; Prado, F.; Rapisarda, V.; Rodríguez-Montelongo, L. Cellular damage induced by a sequential oxidative treatment on *Penicillium digitatum*. *J. Appl. Microbiol.* **2010**, *109*, 1441–1449. [CrossRef]
31. Di Rienzo, J.A.; Casanoves, F.; Balzarini, M.G.; Gonzalez, L.; Tablada, M.; Robledo, C.W.; InfoStat Versión 2020. Centro de Transferencia InfoStat, FCA, Universidad Nacional de Córdoba, Argentina. Available online: <http://www.infostat.com.ar> (accessed on 4 November 2024).
32. Chieng, B.W.; Loo, Y.Y. Synthesis of ZnO nanoparticles by modified polyol method. *Mater. Lett.* **2012**, *73*, 78–82. [CrossRef]
33. Jillani, S.; Jelani, M.; Hassan, N.U.; Ahmad, S.; Hafeez, M. Synthesis, characterization and biological studies of copper oxide nanostructures. *Mater. Res. Express* **2018**, *5*, 045006. [CrossRef]
34. Jyoti, K.; Baunthiyal, M.; Singh, A. Characterization of silver nanoparticles synthesized using *Urtica dioica* Linn. leaves and their synergistic effects with antibiotics. *J. Radiat. Res. Appl. Sci.* **2016**, *9*, 217–227.
35. Sizochenko, N.; Mikolajczyk, A.; Syzochenko, M.; Puzyn, T.; Leszczynski, J. Zeta potentials (ζ) of metal oxide nanoparticles: A meta-analysis of experimental data and a predictive neural networks modeling. *NanoImpact* **2021**, *22*, 100317. [CrossRef] [PubMed]
36. Tomaszewska, E.; Soliwoda, K.; Kadziola, K.; Tkacz-Szczesna, B.; Celichowski, G.; Cichomski, M.; Szmaja, W.; Grobelny, J. Detection limits of DLS and UV-Vis spectroscopy characterization of polydisperse nanoparticles colloids. *J. Nanomater.* **2013**, *2013*, 313081. [CrossRef]
37. Pallavi, S.S.; Rudayni, H.A.; Bepari, A.; Niazi, S.K.; Nayaka, S. Green synthesis of Silver nanoparticles using *Streptomyces hirsutus* strain SNPGA-8 and their characterization, antimicrobial activity, and anticancer activity against human lung carcinoma cell line A549. *Saudi J. Biol. Sci.* **2022**, *29*, 228–238.
38. Consolo, V.F.; Torres-Nicolini, A.; Alvarez, V.A. Mycosinthesized Ag, CuO and ZnO nanoparticles from a promising *Trichoderma harzianum* strain and their antifungal potential against important phytopathogens. *Sci. Rep.* **2020**, *10*, 20499. [CrossRef]
39. Yassin, M.A.; Elgorban, A.M.; El-Samawaty, A.E.-R.M.; Almunqedhi, B.M. Biosynthesis of silver nanoparticles using *Penicillium verrucosum* and analysis of their antifungal activity. *Saudi J. Biol. Sci.* **2021**, *28*, 2123–2127. [CrossRef]
40. Shammout, M.; Awwad, A. A novel route for the synthesis of copper oxide nanoparticles using *Bougainvillea* plant flowers extract and antifungal activity evaluation. *Chem. Int.* **2021**, *7*, 71–78.
41. Olmedo, G.M.; Cerioni, L.; Sepulveda, M.; Ramallo, J.; Rapisarda, V.A.; Volentini, S.I. Polyhexamethylene guanidine as a fungicide, disinfectant and wound protector in lemons challenged with *Penicillium digitatum*. *Food Microbiol.* **2018**, *76*, 128–134. [CrossRef]
42. Vilanova, L.; Viñas, I.; Torres, R.; Usall, J.; Jauset, A.; Teixidó, N. Infection capacities in the orange-pathogen relationship: Compatible (*Penicillium digitatum*) and incompatible (*Penicillium expansum*) interactions. *Food Microbiol.* **2012**, *29*, 56–66. [CrossRef]
43. Rai, M.; Yadav, A.; Gade, A. Silver nanoparticles as a new generation of antimicrobials. *Biotechnol. Adv.* **2009**, *27*, 76–83. [CrossRef]
44. Erasmus, A.; Lennox, C.L.; Korsten, L.; Lesar, K.; Fourie, P.H. Imazalil resistance in *Penicillium digitatum* and *P. italicum* causing citrus postharvest green and blue mould: Impact and options. *Postharvest Biol. Technol.* **2015**, *107*, 66–76. [CrossRef]
45. Pérez, E.; Blanco, O.; Berreta, C.; Dol, I.; Lado, J. Imazalil concentration for in vitro monitoring of imazalil resistant isolates of *Penicillium digitatum* in citrus packinghouses. *Postharvest Biol. Technol.* **2011**, *60*, 258–262. [CrossRef]
46. Chen, J.-N.; Wu, L.-T.; Song, K.; Zhu, Y.-S.; Ding, W. Nonphytotoxic copper oxide nanoparticles are powerful “nanoweapons” that trigger resistance in tobacco against the soil-borne fungal pathogen *Phytophthora nicotianae*. *J. Integr. Agric.* **2022**, *21*, 3245–3262. [CrossRef]
47. Jian, Y.; Chen, X.; Ahmed, T.; Shang, Q.; Zhang, S.; Ma, Z.; Yin, Y. Toxicity and action mechanisms of silver nanoparticles against the mycotoxin-producing fungus *Fusarium graminearum*. *J. Adv. Res.* **2022**, *38*, 1–12. [CrossRef] [PubMed]
48. Radhakrishnan, V.S.; Mudiam, M.K.R.; Kumar, M.; Dwivedi, S.P.; Singh, S.P.; Prasad, T. Silver nanoparticles induced alterations in multiple cellular targets, which are critical for drug susceptibilities and pathogenicity in fungal pathogen (*Candida albicans*). *Int. J. Nanomed.* **2018**, *13*, 2647–2663. [CrossRef]
49. Carlson, C.; Hussain, S.M.; Schrand, A.M.; Braydich-Stolle, L.K.; Hess, K.L.; Jones, R.L.; Schlager, J.J. Unique Cellular Interaction of Silver Nanoparticles: Size-Dependent Generation of Reactive Oxygen Species. *J. Phys. Chem. B* **2008**, *112*, 13608–13619. [CrossRef]
50. Iliger, K.S.; Sofi, T.A.; Bhat, N.A.; Ahanger, F.A.; Sekhar, J.C.; Elhendi, A.Z.; Al-Huqail, A.A.; Khan, F. Copper nanoparticles: Green synthesis and managing fruit rot disease of chilli caused by *Colletotrichum capsici*. *Saudi J. Biol. Sci.* **2021**, *28*, 1477–1486. [CrossRef]
51. Saqib, S.; Zaman, W.; Ayaz, A.; Habib, S.; Bahadur, S.; Hussain, S.; Muhammad, S.; Ullah, F. Postharvest disease inhibition in fruit by synthesis and characterization 501 of chitosan iron oxide nanoparticles. *Biocatal. Agric. Biotechnol.* **2020**, *28*, 101729. [CrossRef]
52. Sajjad, H.; Sajjad, A.; Haya, R.T.; Khan, M.M.; Zia, M. Copper oxide nanoparticles: In vitro and in vivo toxicity, mechanisms of action and factors influencing their toxicology. *Comp. Biochem. Physiol. Part C Toxicol. Pharmacol.* **2023**, *271*, 109682. [CrossRef]
53. Noga, M.; Milan, J.; Frydrych, A.; Jurowski, K. Toxicological aspects, safety assessment, and green toxicology of silver nanoparticles (AgNPs)—Critical review: State of the art. *Int. J. Mol. Sci.* **2023**, *24*, 5133. [CrossRef]
54. Uthaman, A.; Lal, H.M.; Thomas, S. Fundamentals of silver nanoparticles and their toxicological aspects. In *Polymer Nanocomposites Based on Silver Nanoparticles: Synthesis, Characterization and Applications*; Springer: Berlin/Heidelberg, Germany, 2021; pp. 1–24.

Disclaimer/Publisher’s Note: The statements, opinions and data contained in all publications are solely those of the individual author(s) and contributor(s) and not of MDPI and/or the editor(s). MDPI and/or the editor(s) disclaim responsibility for any injury to people or property resulting from any ideas, methods, instructions or products referred to in the content.